

Mechanical Properties of ZnO Nanowires

Baomei Wen,¹ John E. Sader,² and John J. Boland^{1,*}

¹*School of Chemistry and Centre for Research on Adaptive Nanostructures and Nanodevices (CRANN), Trinity College Dublin, Dublin 2, Ireland*

²*Department of Mathematics and Statistics, The University of Melbourne, Victoria, 3010, Australia*

(Received 26 June 2008; published 21 October 2008)

Semiconductor nanowires are unique as functional building blocks in nanoscale electrical and electromechanical devices. Here, we report on the mechanical properties of ZnO nanowires that range in diameter from 18 to 304 nm. We demonstrate that in contrast to recent reports, Young's modulus is essentially independent of diameter and close to the bulk value, whereas the ultimate strength increases for small diameter wires, and exhibits values up to 40 times that of bulk. The mechanical behavior of ZnO nanowires is well described by a mechanical model of bending and tensile stretching.

DOI: [10.1103/PhysRevLett.101.175502](https://doi.org/10.1103/PhysRevLett.101.175502)

PACS numbers: 62.25.-g

The mechanical properties of nanomaterials are of considerable interest given the potential applications of nanostructures in electronic and electromechanical devices. A knowledge of these mechanical properties is essential for designing, manufacturing, and operating such devices. Quasi-one-dimensional nanostructures are particularly interesting since they possess unique properties associated with their highly anisotropic geometry together with finite size effects and their roles in the exclusion of defect from these materials. Nanowires (NWs) represent excellent model systems to investigate this size dependence, particularly the ability to tune the radius over a continuous range to investigate the manner in which their properties approach those of the bulk as a function of shape and size.

ZnO is a promising material with potential applications as a highly sensitive atomic force microscopy (AFM) cantilever [1], a candidate material for flat panel displays and LEDs, and a transparent conducting oxide material and gas sensor [2]. These applications exploit the unique properties of this material. ZnO is a semiconductor, with a direct wide band gap of 3.37 eV and a large exciton binding energy of 60 meV. It is also highly piezoelectric owing to its noncentrosymmetric structure, which is a key in building electromechanically coupled sensors and transducers. Finally, ZnO is a biosafe and biocompatible material thus opening up potential bioapplications. Although ZnO nanowires have been synthesized successfully by vapor transport [3,4] or wet chemistry routes [5,6], and characterized optically and electrically, much less is known about their mechanical properties. Whereas the bulk mechanical properties of ZnO are well established, the reported values of the elastic modulus of nanowires or nanobelts are widely scattered with reported values that are significantly less than the bulk value: 58 GPa by a mechanical resonance experiment [7], 52 GPa by dual-mode resonance [8], (31 ± 2) GPa by a three-point bending test [9], and (29 ± 8) GPa by a single clamped nanowire bending experiment [10]. More recently, Chen *et al.* [11] have observed a size dependent Young's modulus using an electric-field-

induced resonance flexure method. The Young's modulus of ZnO nanowires was measured [11] to be 140 GPa for NWs with diameters larger than 200 nm and up to 220 GPa for NWs with a diameter down to 50 nm. There is at present no general consensus on how size effects the mechanical properties of ZnO nanowires. Clearly, a better understanding of ZnO NW mechanical behavior is critical before these nanoscale materials can be successfully incorporated into electromechanical devices and sensors.

Mechanical measurements of individual nanowire are a challenge, principally because of the difficulties in performing standard tensile or bending tests on freestanding nanoscale objects. Several approaches have been developed including the use of electrically and mechanically excited resonance flexure [11] and nanostressing stage within scanning electron microscope (SEM) [12], transmission electron microscope (TEM) [13,14], and atomic force microscope (AFM) [15–23] measurements. The latter is most popular due to its high spatial resolution and force-sensing capabilities. In this work we report on the mechanical properties of ZnO nanowires that range in diameter from 18 to 304 nm using an AFM lateral bending technique developed very recently [21], which allows the full spectrum of mechanical properties to be measured, including the elastic modulus, plasticity, ultimate strength, and failure. We demonstrate that Young's modulus of these nanowires is essentially independent of diameter. In contrast to recent reports [11] the average value of the modulus is very close to that reported for its bulk and thin-film values (about 144 GPa). On the other hand the ultimate strengths are up to 40 times that of bulk for smaller-diameter nanowires and ZnO nanowires exhibit brittle failure without measurable plastic deformation.

ZnO nanowires were synthesized by a mild solvothermal route using a thin nucleation layer of nanostructural ZnO deposited on thermally oxidized Si substrates under an Ar and O₂ atmosphere by room temperature direct current (DC) magnetron reactive sputtering, similar to that reported earlier [24]. The reaction was performed in a sealed

autoclave filled with equimolar ethanol solutions (0.001M) of zinc nitrate hexahydrate ($\text{Zn}(\text{NO}_3)_2 \cdot 6\text{H}_2\text{O}$) and hexamethylenetetramine ($\text{C}_6\text{H}_{12}\text{N}_4$, HMTA) by suspending the Si substrates containing the ZnO seed layer. The typical reaction time is 24–48 h at 80 °C. Cetyltrimethylammoniumbromide (CTAB) was used as the modifying and controlling agent for tuning the diameter of ZnO nanowires. The high-resolution TEM image and SAED pattern in Fig. 1(a) show that these nanowires have perfect single crystalline wurtzite structure along [0001] growth direction. The inset shows a low magnification scanning electron microscopy image of ZnO nanowires with lengths of many micrometers and diameters of around 20 nm.

To perform lateral bending tests, ZnO nanowires were sonicated off the supporting substrate and dispersed in ethanol, then deposited on a prepatterned substrate which contains well-defined trench patterns fabricated by focus-ion-beam milling. Trenches have 400–500 nm depth and various widths the latter chosen according to the diameter of nanowires. Typically, the ratio of trench width to nanowire diameter is around 30 times, which eliminates wire droop and minimizes the role of the clamps in the lateral AFM bending experiments. Nanowires were subsequently double-clamped at the trench edges by electron beam induced deposition of Pt lines, with the pinning points deposited as close to the edge as possible to accurately define the spanning length and to eliminate wire-substrate friction at the clamps during AFM bending manipulations [see Fig. 1(b)]. Two types of well-calibrated rectangular cantilevers with average normal force constants of 3 N/m (75 kHz) and 40 N/m (300 kHz) were used in the bending experiments. AFM lateral manipulations were performed using a Digital Instruments Nanoman System with closed-loop x - y - z scanner. The normal and lateral force signals were recorded as a function of displacement using a Labview-based program. The lateral force data was analyzed exclusively since the normal force just contributes less than 5% of the total force signal. A more detailed description of the manipulation and tip calibration procedures can be found elsewhere [21].

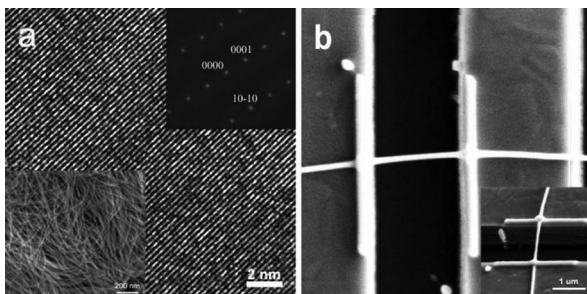


FIG. 1. (a) A high-resolution TEM image of ZnO nanowire. The insets are a selected-area electron diffraction pattern corresponding to the 0001 growth direction, and a SEM image. (b) Nanowire bridging the trenches double clamped at the trench edges by electron beam induced deposition of Pt lines. The inset shows a rotated view of the same wire and pinning geometry.

Nanowires were imaged in tapping mode before each manipulation, then the cantilever oscillation was switched off, and the lateral bending test was performed in contact mode along a trajectory that intersects the middle of the suspended wire. Figure 2 shows a typical set of F - d curves for a 288 nm diameter ZnO nanowire and the corresponding AFM images before bending and after failure. The resulting F - d curve [Fig. 2(c)] shows that during manipulation the lateral force is essentially zero until contact is established between tip and nanowire. Subsequently, the force F increases approximately linearly with the wire displacement, reflecting the bending deformation of the wire. Finally, a sharp force-drop is observed that is associated with wire failure; this is immediately confirmed by the later AFM image in Fig. 2(b). The wire is elastically deformed up to a displacement of 140 nm, followed by brittle failure. No plastic deformation is observed. The mechanical properties over the entire elastic range can be well described by a generalized model [red curve in Fig. 2(c)] which provides an accurate measurement of the Young's modulus E and allows the yield point to be identified in nanowire systems [25].

Figure 3 shows a F - d curve of the corresponding bending manipulation for a 18 nm diameter ZnO nanowire. The applied force F initially increases linearly with the wire displacement, and then increases much more rapidly at larger displacement, exhibiting an approximately cubic

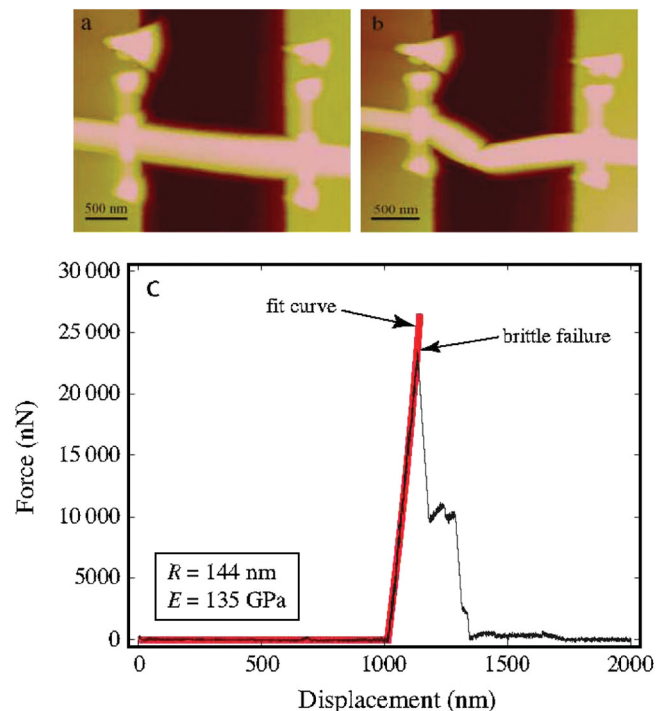


FIG. 2 (color). (a) and (b) Tapping-mode AFM images of a 144 nm radius ZnO nanowire before bending and after brittle failure. (c) F - d curve recorded during the manipulation by AFM tip-induced lateral bending of a 144 nm ZnO nanowire (in black) and fit of F - d curve to the generalized formula, which yield a Young's modulus of 135 GPa (in red).

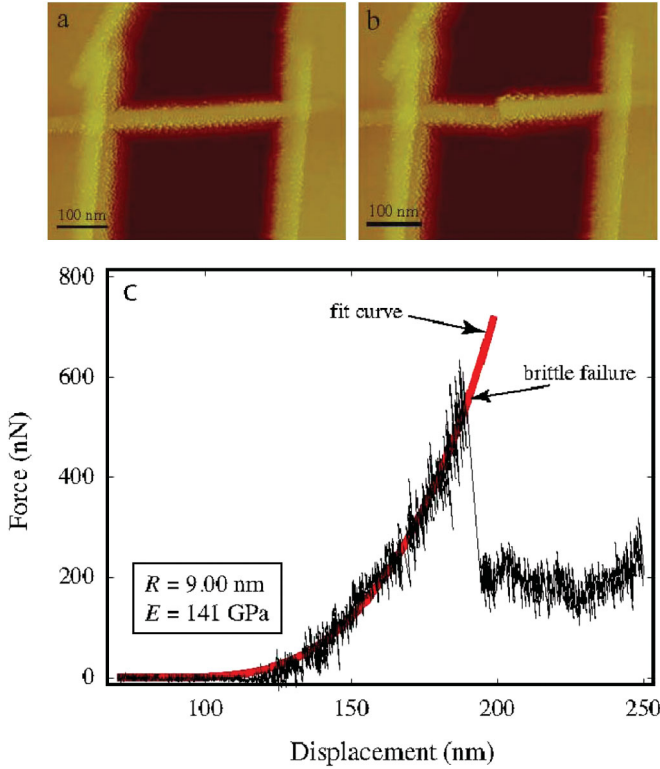


FIG. 3 (color). (a) and (b) Tapping-mode AFM images of a 9 nm radius ZnO nanowire before bending and after brittle failure. (c) F - d curve recorded during the manipulation by AFM tip-induced lateral bending of a 9 nm nanowire (in black) and fit of the F - d curve to the generalized formula, which yield a Young's modulus of 141 GPa (in red).

dependence. At these larger displacements an axial tensile force is inherently induced because of the stretching of the wire, which affects the total stress experienced by the beam, resulting in an enhancement of its rigidity [26]. The 18 nm wire can be elastically deformed up to 72 nm before brittle failure.

The mechanical behaviors of both the 18 nm and 288 nm wires are well described by the mechanical model described previously that accounts for both bending and tensile stretching. The solution is given by [25]

$$F_{\text{center}} = \frac{192EI}{L^3} f(\alpha) \Delta z_{\text{center}}, \quad (1)$$

where F_{center} is the applied force to the center of the wire, E is the Young's modulus of the wire, Δz_{center} is the resulting displacement of the wire at the load point, $I = \pi R^4/4$ is the moment of inertia for a cylindrical wire, and L is the wire length. The function $f(\alpha)$ is defined

$$f(\alpha) = \frac{\alpha}{48 - \frac{192 \tanh(\sqrt{\alpha}/4)}{\sqrt{\alpha}}}, \quad (2)$$

where α is related to the displacement Δz_{center} of the wire by

$$\alpha = \frac{6\varepsilon(140 + \varepsilon)}{350 + 3\varepsilon}, \quad \varepsilon = \left(\frac{2\Delta z_{\text{center}}}{R} \right)^2. \quad (3)$$

Note that inducement of a tensile force along the beam at large displacements enhances the wire stiffness, i.e., $f(\alpha) \geq 1$. An approximate solution to Eq. (1)–(3) can be developed in which the approximate linear and cubic dependence found in Figs. 2 and 3 is explicitly seen [25].

The generalized model in Eqs. (1)–(3) was applied to 51 individual ZnO nanowires that range in diameter from 18 to 304 nm. Figure 4(a) shows that the measured Young's modulus is essentially independent of wire diameter over the range investigated. The average value of the modulus is 133 ± 15 GPa, which is very close to that of the bulk ZnO (144 GPa along [0001]), computed from elastic constants from the literature [27]. These values are significantly larger than the 21–58 GPa values previously reported for ZnO nanowires and nanobelts [7–10]. Moreover, we find no evidence to support the dramatic increase in stiffness of over 200% the bulk value for sub 120 nm wires, reported by Chen *et al.* [11]. In comparison with previously reported results and particularly those employing resonance flexure methods [11], the data presented here show a much lower spread of values. The propagation of errors in the present method is due primarily due to uncertainties in the physical dimensions of the wire and AFM cantilever/tip, and the photodiode sensitivity; the maximum relative errors in the formulas used to estimate the Young's modulus and ultimate strength are no more than a few percent [25].

The ultimate strengths of the ZnO wires were determined using [28]

$$\sigma_y = \frac{F_{\text{center}}L}{2\pi R^3} g(\alpha), \quad (4)$$

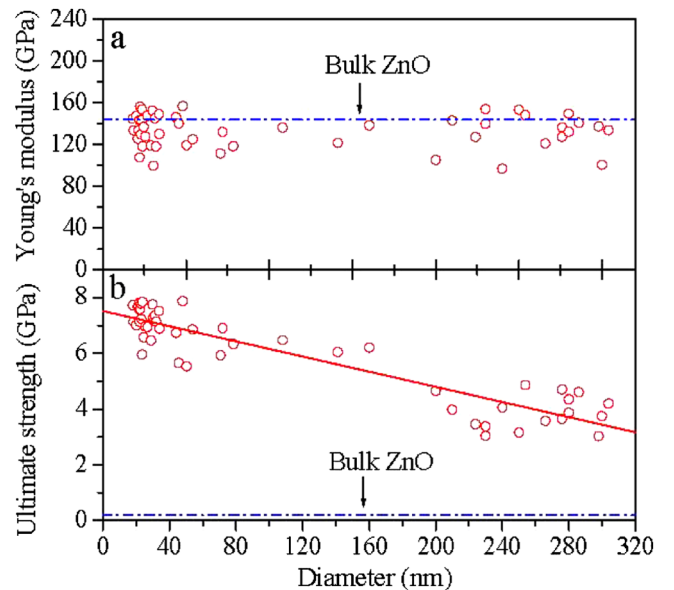


FIG. 4 (color online). (a) Young's modulus and (b) ultimate strength values obtained from experiments for ZnO nanowires. The bulk values are shown in blue dash-dot lines.

where

$$g(\alpha) = \frac{4}{\sqrt{\alpha}} \tanh\left(\frac{\sqrt{\alpha}}{4}\right) + \left(\frac{2 + \cosh(\sqrt{\alpha}/2) - 6\frac{\sinh(\sqrt{\alpha}/2)}{\sqrt{\alpha}}}{\alpha \cosh^2(\sqrt{\alpha}/4)}\right)^{1/2} \quad (5)$$

and found to be diameter dependent, with average values of 6.99 ± 0.67 GPa and 3.90 ± 0.59 GPa for small (30 nm) and large (250 nm) diameter nanowires, respectively. The strength data is shown in Fig. 4(b) and reveal a general strengthening of the wire at smaller diameters. These measured values are much higher than that for bulk ZnO, which is typically smaller than 200 MPa [29], and that of small diameter nanowires is substantially higher than the reported 3.7–5.5 GPa range in the literature. This is similar to measurements reported for Si nanowires, exhibiting elastic fracture behavior with a limit stress approaching the ideal strength. The increased ultimate strength of ZnO nanowires compared to the bulk likely results from a reduction in the number of defects in the nanowire, a phenomenon that is common and indeed expected in nanoscale systems.

The ability of a material to deform elastically prior to failure is an important factor for mechanical applications. Smaller-diameter wires are remarkably flexible and capable of an elastic deformation up to 4–5 times their diameters prior to failure [see Fig. 3(c)]. The excellent resilience and the ability to store elastic energy in these nanowires confirm their potential for applications as sensors and electromechanical oscillators.

The differences in the mechanical properties reported here compared to those in the literature [7–11] warrant comment. While Chen *et al.* [11] report an increase in Young's modulus with miniaturization, others report a decrease with values as low as 29 GPa [10], compared with a bulk value of 144 GPa. Prior studies involved NWs attached to *W* tips for (electric-field-induced) resonance measurement [7,8,11] or manipulated as vertically grown wires [10,30]. The clamping, excitation, and energy dissipation mechanisms are not clear in the former, whereas the composition and diameter are not well established at the base of vertically grown wires. The single feature that distinguishes the present technique is the simplicity of the double-clamped configuration and the fact that the clamps were intentionally deposited; their integrity was checked both before and after manipulation experiments. This simple method is direct and robust, and provides unequivocal estimates of both Young's modulus and ultimate strength that are in line with bulk values.

In conclusion, we have performed controlled lateral force AFM measurement of the mechanical properties of ZnO nanowires that have been characterized by HRTEM. We have demonstrated that in contrast to recent reports the modulus is diameter independent and close to the bulk value down to diameters of 18 nm. The ultimate strength

of these materials increases for small diameter wires approaching values of 7.00 GPa, which is consistent with reduced levels of defect incorporation as the materials dimensions are reduced. These wires are also shown to be remarkably resilient exhibiting deformations that approach 5 times the diameter. The excellent mechanical properties demonstrated by these wires suggest that they will be exceptionally useful building blocks in the development of future nanoscale electromechanical devices.

This work was supported by Science Foundation Ireland under Grant 06/IN.1/I106, the Particulate Fluids Processing Centre of the Australian Research Council and by the Australian Research Council Grants Scheme.

*Corresponding author.

jboland@tcd.ie

- [1] Z. Y. Fan and J. G. Lu, *J. Nanosci. Nanotech.* **5**, 1561 (2005).
- [2] M. H. Zhao *et al.*, *Mater. Sci. Eng. A* **409**, 223 (2005).
- [3] M. H. Huang *et al.*, *Adv. Mater.* **13**, 113 (2001).
- [4] J. S. Lee, M. S. Islam, and S. Kim, *Nano Lett.* **6**, 1487 (2006).
- [5] C. H. Lu *et al.*, *Chem. Commun. (Cambridge)* **2006**, 3551.
- [6] L. Vayssieres, *Adv. Mater.* **15**, 464 (2003).
- [7] Y. H. Huang, X. D. Bai, and Y. Zhang, *J. Phys. Condens. Matter* **18**, L179 (2006).
- [8] X. D. Bai *et al.*, *Appl. Phys. Lett.* **82**, 4806 (2003).
- [9] H. Ni and X. D. Li, *Nanotechnology* **17**, 3591 (2006).
- [10] J. H. Song *et al.*, *Nano Lett.* **5**, 1954 (2005).
- [11] C. Q. Chen *et al.*, *Phys. Rev. Lett.* **96**, 075505 (2006).
- [12] M. F. Yu *et al.*, *Science* **287**, 637 (2000).
- [13] P. Poncharal *et al.*, *Science* **283**, 1513 (1999).
- [14] R. P. Gao *et al.*, *Phys. Rev. Lett.* **85**, 622 (2000).
- [15] E. W. Wong, P. E. Sheehan, and C. M. Lieber, *Science* **277**, 1971 (1997).
- [16] J. P. Salvetat *et al.*, *Phys. Rev. Lett.* **82**, 944 (1999).
- [17] A. Kis *et al.*, *Adv. Mater.* **15**, 733 (2003).
- [18] T. W. Tomblor *et al.*, *Nature (London)* **405**, 769 (2000).
- [19] E. D. Minot *et al.*, *Phys. Rev. Lett.* **90**, 156401 (2003).
- [20] X. D. Li *et al.*, *Nano Lett.* **3**, 1495 (2003).
- [21] B. Wu, A. Heidelberg, and J. J. Boland, *Nature Mater.* **4**, 525 (2005).
- [22] B. Wu *et al.*, *Nano Lett.* **6**, 468 (2006).
- [23] L. T. Ngo *et al.*, *Nano Lett.* **6**, 2964 (2006).
- [24] B. M. Wen, Y. Z. Huang, and J. J. Boland, *J. Phys. Chem. C* **112**, 106 (2008).
- [25] A. Heidelberg *et al.*, *Nano Lett.* **6**, 1101 (2006).
- [26] L. D. Landau and E. M. Lifshitz, *Theory of Elasticity* (Pergamon, Oxford, 1970).
- [27] H. Wern, *Single Crystal Elastic Constants and Calculated Bulk Properties* (LV, Berlin, Germany, 2004).
- [28] J. M. Gere and S. P. Timoshenko, in *Mechanics of Materials* (PWS-KENT, Boston, MA, 1990), Chap. 5.1.8.
- [29] C. Lu., R. Danzer, and F. D. Fischer, *Phys. Rev. E* **65**, 067102 (2002).
- [30] S. Hoffmann *et al.*, *Nanotechnology* **18**, 205503 (2007).